Metaxial correction of fractional Fourier transformers

Kurt Bernardo Wolf and Guillermo Krötzsch

Centro de Ciencias Físicas, Universidad Nacional Autónoma de México, Apartado Postal 48-3, 62251 Cuernavaca, Morelos, México

Received June 29, 1998; revised manuscript received October 8, 1998; accepted November 13, 1998

We study fractional Fourier transformation in the metaxial regime of geometric optics. Two commonly used optical arrangements that perform fractional Fourier transformation are a symmetric thick lens and a length of graded-index waveguide. By means of Lie methods in phase space, we can correct some of their aberrations: for the first, through deforming the lens surfaces to a polynomial shape, and for the second, by warping the output screen at the end of the waveguide. We correct the planar cases to third, fifth, and seventh aberration orders; checks are provided on the convergence of aberration series in phase space. We add some comments on the usefulness of these corrected devices for fractional transformers in scalar wave optics. [S0740-3232(99)00904-7]

OCIS codes: 070.2590, 080.1010, 080.2720.

1. INTRODUCTION: FRACTIONAL FOURIER TRANSFORM

Fourier transformation is a rotation of phase space between the canonical coordinates of position and momentum. In mechanics this occurs when the system evolves in a harmonic-oscillator potential; there the phase-space plane rotates rigidly about the origin, so its coordinates mix linearly. In optics, however, this transformation is possible only in the small neighborhood of the design ray where the paraxial regime applies, because optical phase space constrains the momentum coordinates (i.e., ray direction) to a sphere. The optical Fourier transformation *must* be nonlinear. In Ref. 1 one of the authors proposed a proper, canonical Fourier transformation of optical phase space by means of a similarity map from the phase space of geometric and wave optics onto that of classical and quantum mechanics,[2] but no concrete arrangement was proposed.

Fourier transformations in optics also meet the impediment that no true harmonic-oscillator potential exists. Of course, in the paraxial regime, Fourier transformers are easily built between the input and output screens at the focal points of a lens, or by an appropriate length of an axisymmetric graded-index waveguide, with radial index profiles of any negative curvature. In this paper we analyze lens- and waveguide-based Fourier transformers beyond the paraxial regime by using Lie–Hamilton phase-space techniques, which are reviewed in Section 2. Our purpose is to correct such transformers to map phase space as linearly as possible in a neighborhood of the design ray as large as possible. Two correction tactics are explored: in Section 3 we consider the symmetric lens arrangement with polynomial refracting lines, and in Section 4 we propose waveguides with a warped output screen. Such systems will perform better for larger screens and angles. Finally, Section 5 adds some comments on the relevance of these conclusions to the design of wave-optical fractional Fourier transformers.

In spite of their conceptual terseness, Lie aberration expansions do not seem to have actually been used for nonimaging optical systems. The paraxial part is the first-order approximation by an unperturbed quadratic Hamiltonian that can be easily factored off; this places the analysis of aberrations in the interaction picture of quantum mechanics. We confirm the convergence of the Lie aberration expansion to seventh order of the two systems under consideration in a usefully large region of phase space. Through the symbolic computation program MEXLIE developed by the authors,[3] the aberration coefficients are found as a function of all the parameters of the system; recursive algorithms are found here that correct the lens and waveguide arrangements with one parameter each. We do not attempt in this paper to design a "best" Fourier transformer, presumably obtained by multiparameter optimization algorithms with several correction tactics, because such a solution would surely turn out to be numerical. By correcting a single parameter at each aberration order, we can follow the process analytically and detect the possibilities and the limitations of each minimization tactic. We study flat, two-dimensional (2-D) optical arrangements, where the optical and screen axes (z, q) provide Cartesian-space coordinates. The phase space (p, q) of 2-D systems is also 2-D and can be plotted conveniently on a plane.

2. LIE–HAMILTON ABERRATIONS OF PHASE SPACE

Geometric optical phase space in a 2-D world is a 2-D symplectic manifold whose points are rays with a canonical coordinate of position $q \in \mathbb{R}$, its intersection with the screen, and its conjugate momentum $p = n \sin\theta \in (-n, n)$, where n is the refractive index and θ is the angle between the ray and the optical axis.[4] Optical phase space is composed of two coordinate charts that are strips $|p| < n$ in $(p, q) \in \mathbb{R}^2$, corresponding to rays that cross the screen in the forward ($|\theta| < \frac{1}{2}\pi$) and backward directions. The two strips are identified at their edges $\theta = \pm\frac{1}{2}\pi$. Optical phase space is thus globally distinct from the phase space $\mathbb{R}^2$ of one-dimensional mechanics, where the momentum coordinate is mass times velocity and unbounded (locally, the two coincide within each strip $|p| < n$ as any two symplectic manifolds). The metaxial model of geometric optics replaces the forward strip of phase space by the $\mathbb{R}^2$ symplectic plane and represents optical elements by transformations of this plane.

Functions on symplectic manifolds are endowed with the Poisson bracket composition

$$\{F(p,q),\ G(p,q)\} = \frac{\partial F(p,q)}{\partial q}\frac{\partial G(p,q)}{\partial p} - \frac{\partial F(p,q)}{\partial p}\frac{\partial G(p,q)}{\partial q}, \quad (2.1a)$$

which is bilinear and antisymmetric, satisfies the Jacobi identity (i.e., fulfills the properties of a Lie bracket), and obeys the Leibniz rule of derivation. By the latter the Poisson bracket of any two functions can be determined from

$$\{q, p\} = 1, \qquad \{q, 1\} = 0, \qquad \{p, 1\} = 0. \quad (2.1b)$$

Transformations of a symplectic manifold $\mathcal{G}\{\mathbf{A};\ \mathbf{M}\}$: $(p,q) \to (p'(p,q), q'(p,q))$ that preserve Eqs. (2.1) (the Heisenberg–Weyl Lie algebra, i.e., $\{q', p'\} = 1$, etc.) are called canonical. Canonicity implies that phase-space volume elements are preserved: $\mathrm{d}q'\mathrm{d}p' = \mathrm{d}q\mathrm{d}p$. Thus rays are neither created nor destroyed but only transformed. (In two dimensions the volume-preservation property conversely implies canonicity.) Transformations of optical phase space produced by passive optical elements are necessarily canonical.

Transformations that leave the design ray invariant [i.e., $(p'(0,0),\ q'(0,0)) = (0,0)$] are amenable to Taylor expansion in powers of p and q.[5] Then, because the Poisson bracket (2.1a) between two polynomials in (p, q) of degrees n and m is a polynomial of degree $n + m - 2$, we can consistently truncate all Taylor-expanded functions to some integer polynomial degree $a \geqslant 1$. This polynomial ring in phase space with the Poisson bracket operation constitutes the ath-order aberration model of geometric optics. The metaxial model is the nested sequence of ath-order aberration models whose kernel is the $a = 1$ paraxial model. The latter allows only linear transformations of unit determinant, represented by 2×2 real matrices.

Paraxial fractional Fourier transformers $\mathcal{G}\{\mathbf{0};\ \mathbf{\Phi}(\alpha)\}$ are characterized by the rotation matrices

$$\mathbf{\Phi}(\alpha) = \begin{bmatrix} \cos\alpha & -\sin\alpha \\ \sin\alpha & \cos\alpha \end{bmatrix}. \quad (2.2)$$

Their action on $\mathbb{R}^2$ phase space is through the inverse of the matrix:

$$\mathcal{G}\{\mathbf{0};\ \mathbf{\Phi}(\alpha)\}\begin{pmatrix} p \\ q \end{pmatrix} = [\mathbf{\Phi}(\alpha)]^{-1}\begin{pmatrix} p \\ q \end{pmatrix} = \begin{pmatrix} p_\alpha \\ q_\alpha \end{pmatrix} = \begin{pmatrix} p\cos\alpha + q\sin\alpha \\ -p\sin\alpha + q\cos\alpha \end{pmatrix}. \quad (2.3)$$

For $\alpha > 0$ this is a clockwise rotation of the phase plane around the origin, as shown in Fig. 1. The origin represents the design ray through the optical axis of the system. Fractional Fourier transformations evidently form a group with composition rule $\mathbf{\Phi}(\alpha_1)\mathbf{\Phi}(\alpha_2) = \mathbf{\Phi}(\alpha_1 + \alpha_2)$. The identity element is $\mathbf{\Phi}(0) = \mathbf{1}$, and $[\mathbf{\Phi}(\alpha)]^{-1} = \mathbf{\Phi}(-\alpha)$. The (original, well-known) Fourier transformation corresponds to $\alpha = \frac{1}{2}\pi = 90°$, which outputs images of the incoming ray directions. The element $\alpha = \pm\pi$ is a perfect (inverted) imager.

The previous equations raise the issue of the physical units of phase space. In quantum mechanics there is a fundamental unit of action (momentum×length), the reduced Planck constant $\hbar = h/2\pi$, which measures the area of phase space and provides the relative scale of the position and momentum uncertainty from the well-known Lie commutator $[\hat{Q},\ \hat{P}] = i\hbar\mathbf{1}$. In natural units $\hbar$ is assigned the value 1. Paraxial wave optics uses the same commutator, but with a third, living operator on the right-hand side, $\hat{\Lambda}$ (times i), whose eigenvalues are the reduced wavelengths $\lambda/2\pi \in \mathbb{R} - \{0\}$ different from zero; the momentum, as the refractive index, is dimensionless, and positions have units of length $\lambda/2\pi$. Although geometric optics is commonly regarded as the $\lambda \to 0$ limit of wave optics, its fundamental definitions (2.1) and derivative relations such as Eqs. (2.2) and (2.3) are dimensionless. Following the lead of wave optics, we can write $q = q^*/l$, where l is a fundamental length of the system, 15 cm say, and q^* is in centimeters. On replacing q by q^*, we obtain $\{q^*, p\} = l$ in Eq. (2.1b), and in Eq. (2.2) we obtain a factor of l in the lower left corner of the matrix and a factor of l^{-1} in the upper right corner, which render the appropriate units for p_α (dimensionless) and q^*_α (of l) in Eq. (2.3).

We now recall the Lie–Hamilton aberration expansion of nonlinear canonical transformations. A metaxial fractional Fourier transform is a canonical map of phase space whose generic form is

$$\mathcal{F}(\alpha) = \mathcal{G}\{\mathbf{A};\ \mathbf{\Phi}(\alpha)\} = \mathcal{G}\{\mathbf{A};\ \mathbf{1}\}\mathcal{G}\{\mathbf{0};\ \mathbf{\Phi}(\alpha)\}, \quad (2.4)$$

where the paraxial part is the fractional Fourier transformation (2.2) and (2.3) and $\mathbf{A}$ characterizes the nonlinear aberration part. This is an ordered product of Lie–Poisson operators obtained from Eq. (2.1) as[4–6]

$$\mathcal{G}\{\mathbf{A};\ \mathbf{1}\} = \cdots \times \exp\{A_3, \circ\}\exp\{A_{5/2}, \circ\}\exp\{A_2, \circ\} \times \exp\{A_{3/2}, \circ\}, \quad (2.5a)$$

$$\exp\{A_k, \circ\} = \mathbf{1} + \{A_k, \circ\} + \frac{1}{2!}\{A_k, \{A_k, \circ\}\} + \cdots, \quad (2.5b)$$

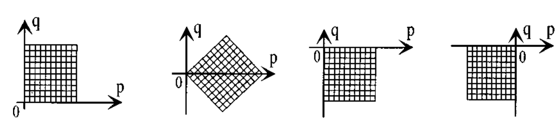

Fig. 1. Paraxial fractional Fourier transformations are rigid rotations of the phase plane around its origin, the optical center corresponding to the design ray, shown here for $\alpha = 0$, $\frac{1}{4}\pi$, $\frac{1}{2}\pi$ (*the* Fourier transform), and π (a perfect, inverted imager).

$$\{A_k, \circ\} = \frac{\partial A_k(p,q)}{\partial q}\frac{\partial}{\partial p} - \frac{\partial A_k(p,q)}{\partial p}\frac{\partial}{\partial q}, \tag{2.5c}$$

where the $A_k(p, q)$ are aberration polynomials of integer homogeneous degree $2k$ in the coordinates of phase space, given as

$$A_k(p,q) = \sum_{m=-k}^{k} A_m^k p^{k+m} q^{k-m}. \tag{2.6}$$

The coefficients $\{A_m^k\}_{m=-k}^k$ are (for two dimensions) the $2k+1$ Lie–Hamilton aberration coefficients of rank k (integer or half-integer); the corresponding aberration order is $a = 2k - 1$. Note that these coefficients are distinct from the Seidel aberration coefficients used in classical works such as that of Buchdahl.[7] [The paraxial part (2.3) can also be written in this manner for $k = 1$ with $\mathcal{G}\{\mathbf{0}; \mathbf{\Phi}(\alpha)\} = \exp(\alpha\frac{1}{2}\{p^2 + q^2, \circ\})$.] As the 2-vector (2.3) of phase-space coordinates transforms with (the transpose of) a matrix $\mathbf{M}$, the column $(2k+1)$-vector of aberration coefficients $\{A_m^k\}_{m=-k}^k$ transforms with the $(2k+1)$-dimensional representation matrix $\mathbf{D}^{(k)}(\mathbf{M})$.

The composition between two generic transformations (2.4) has the form

$$\mathcal{G}\{\mathbf{A};\mathbf{M}\}\mathcal{G}\{\mathbf{B};\mathbf{N}\} = \mathcal{G}\{\mathbf{A} \sharp \mathbf{D}(\mathbf{M})\mathbf{B}; \mathbf{MN}\}, \tag{2.7a}$$

where $\sharp$ is a Baker–Campbell–Hausdorff *gato* product and $\mathbf{D}(\mathbf{M})$ is a block-diagonal representation of the paraxial matrix $\mathbf{M}$,[5,6] with blocks of size $(2k+1)\times(2k+1)$. This product formula has appeared several times in the literature, so we need not repeat it in detail but only note that, for rank k,

$$[\mathbf{A} \sharp \mathbf{D}(\mathbf{M})\mathbf{B}]_k = \mathbf{A}_k + \mathbf{D}^k(\mathbf{M})\mathbf{B}_k + \text{multilinear terms of higher ranks}. \tag{2.7b}$$

When operators (2.5) (and functions) on phase space are Taylor expanded and truncated to degree $a_{\max} = 2k_{\max} - 1$, we have the ath-order aberration group. This has three matrix parameters and the aberration coefficients $\{A_m^k\}$ for $|m| \leqslant k \leqslant k_{\max}$. Canonicity is also redefined for the truncated Taylor series modulo terms of degree greater than $2k$.

A 2-D system whose optical axis is a line of reflection symmetry $(q, \theta) \leftrightarrow (-q, -\theta)$ can contain only those aberrations whose polynomials are symmetric (invariant) under phase-space inversion $(p,q) \leftrightarrow (-p,-q)$. Since polynomials of half-integer rank k are odd under inversion, this symmetry entails the selection rule allowing only integer ranks k and odd aberration orders (third, fifth, seventh, etc.).

The generic third-order aberration polynomial (of rank $k = 2$) is

$$A_2(p,q) = A_2^2 p^4 + A_1^2 p^3 q + A_0^2 p^2 q^2 + A_{-1}^2 p q^3 + A_{-2}^2 q^4. \tag{2.8}$$

The action on phase space of the pure aberration factor $\mathcal{G}\{\mathbf{A};\mathbf{1}\}$ of Eq. (2.5a), truncated to the same order, is then

$$\begin{aligned}\mathcal{G}\{\mathbf{A};\mathbf{1}\}\begin{pmatrix}p\\q\end{pmatrix} &\simeq (1 + \{A_2, \circ\})\begin{pmatrix}p\\q\end{pmatrix}\\ &= \begin{pmatrix}p + A_1^2 p^3 + 2A_0^2 p^2 q + 3A_{-1}^2 p q^2 + 4A_{-2}^2 q^3\\ q - 4A_2^2 p^3 - 3A_1^2 p^2 q - 2A_0^2 p q^2 - A_{-1}^2 q^3\end{pmatrix}\\ &= \begin{pmatrix}p_A^{[3]}(p,q)\\ q_A^{[3]}(p,q)\end{pmatrix},\end{aligned} \tag{2.9}$$

which is canonical to third degree, i.e., disregarding terms of fifth degree and higher. There are five independent third-order aberrations A_m^2, $m = 2, 1, 0, -1, -2$, identified as (Lie–Hamilton) spherical aberration, coma, curvature of field/astigmatism, distortion, and pocus (defocus; cf. Ref. 6), respectively. The fractional Fourier transformer (2.4) first acts with the paraxial part (2.3), replacing (p, q) by (p_α, q_α), and then with the aberration part that is present. To use relation (2.9) alone therefore corresponds (in the familiar setting of perturbation mechanics) to working in the interaction frame of the Hamiltonian system, i.e., in the frame that rotates with Fig. 1. All subsequent figures will be referred to this interaction frame for simpler inspection.

To third aberration order (in the interaction frame), the fractional Fourier transform maps of the (straight) coordinate axes $(p, 0)$ and $(0, q)$ are the cubic curves

$$\begin{aligned} p_A^{[3]}(p,0) &= p + A_1^2 p^3, & p_A^{[3]}(0,q) &= 4A_{-2}^2 q^3,\\ q_A^{[3]}(p,0) &= -4A_2^2 p^3, & q_A^{[3]}(0,q) &= q - A_{-1}^2 q^3.\end{aligned} \tag{2.10}$$

An ideal correction would straighten these lines. It may prove impossible, however, with the physically adjustable parameters available, to set all coefficients to zero. This is the case for the arrangements of Sections 3 and 4, where the system has a single adjustable parameter for each aberration order, so we must propose more flexible criteria for a phase-space map to approximate the paraxial fractional Fourier transform.

One criterion that we propose considers the two 2-vectors at (p, q) that are tangent to the image of the Cartesian grid, namely, $\Delta v = (\Delta p, 0)$ and $\Delta w = (0, \Delta q)$, and demands that they remain orthogonal. Thus we forbid slanting of the grid in phase space. By Eqs. (2.10) an uncorrected, aberrating Fourier transformer (in the interaction frame) will map these tangent vectors on

$$\begin{aligned}\Delta v_A(p) &= \begin{pmatrix}1 + 3A_1^2 p^2\\ -12A_2^2 p^2\end{pmatrix}\Delta p,\\ \Delta w_A(q) &= \begin{pmatrix}12A_{-2}^2 q^2\\ 1 - 3A_{-1}^2 q^2\end{pmatrix}\Delta q.\end{aligned} \tag{2.11}$$

These vectors subtend an angle $\omega \neq 1/2\pi$ given by their scalar product

$$\begin{aligned}\Delta v_A \cdot \Delta w_A &= |\Delta v_A||\Delta w_A|\cos\omega\\ &= [12(A_{-2}^2 q^2 - A_2^2 p^2) + 36(A_1^2 A_{-2}^2 + A_2^2 A_{-1}^2)p^2 q^2]\Delta p \Delta q.\end{aligned} \tag{2.12}$$

The first summand is linear in the A_m^2 (and presumably small), whereas the second is quadratic (and much smaller). The image phase space will have no slanting (to third aberration order) when the transformer is corrected to have aberration coefficients such that $A_2^2 = 0 = A_{-2}^2$. But it proves impossible to satisfy this requirement for the lens transformer of Section 3, because zero is outside the physical range of values of the aberration coefficients. The best that we can do is an approximate correction through

$$A_2^2 = A_{-2}^2, \tag{2.13}$$

so that the image grid is orthogonal on at least the quadrant bisectors $p = \pm q$.

Once the system has been corrected to third aberration order, the fifth-order aberrations are subjected to a similar treatment. The polynomial $A_3(p, q)$ now contains seven independent coefficients $\{A_m^3\}_{m=-3}^3$, and the phase-space map is now

$$p_A^{[5]}(p, q) = (1 + \{A_3, \circ\})\left(1 + \{A_2, \circ\} + \frac{1}{2!}\{A_2, \{A_2, \circ\}\}\right)p, \tag{2.14}$$

and correspondingly for $q_A^{[5]}(p, q)$. We assume that the system is corrected to third order and hence has A_m^2 fixed, but the coordinate grid will be mapped now on quintic curves that osculate the previous cubics and whose departure from orthogonality is dominated by the fifth-order spherical aberration and pocus coefficients, A_3^3 and A_{-3}^3. Again the criterion to correct as much as possible for slanting leads to the condition $A_3^3 = A_{-3}^3$. The system thus corrected to fifth order is then introduced into the seventh-order computation, where

$$p_A^{[7]}(p, q) = (1 + \{A_4, \circ\})(1 + \{A_3, \circ\})\left(1 + \{A_2, \circ\} + \frac{1}{2!}\{A_2, \{A_2, \circ\}\} + \frac{1}{3!}\{A_2, \{A_2, \{A_2, \circ\}\}\}\right)p, \tag{2.15}$$

and similarly for $q_A^{[7]}(p, q)$.

3. LENS ARRANGEMENT

A fractional Fourier transformer can be built by placing a lens between the object screen (a line in 2-D optics) and the image (or sensor) screen, as shown in Fig. 2. This arrangement contains three free-propagation intervals, separated by two refracting lines between distinct homogeneous media. We first recall the necessary results for these two basic optical elements, so as to combine them below into a quasi-corrected transformer.

Free propagation by a distance z along the optical axis in a homogeneous medium n is, by elementary geometry, the phase-space transformation

$$(p = n \sin\theta, q) \to (p, q + z \tan\theta) = (p, q + zp/\sqrt{n^2 - p^2}). \tag{3.1a}$$

This is the evolution produced by $\exp(-z\{h, \circ\})$ generated by the free optical Hamiltonian function $h = -\sqrt{n^2 - p^2} = -n \cos\theta$:

$$\mathcal{Z}(z, n) = \exp(z\{\sqrt{n^2 - p^2}, \circ\}) = \cdots \exp\left(\frac{-z}{16n^5}\{p^6, \circ\}\right)\exp\left(\frac{-z}{8n^3}\{p^4, \circ\}\right) \times \exp\left(\frac{-z}{2n}\{p^2, \circ\}\right) \tag{3.1b}$$

$$= \mathcal{G}\{\cdots, Z_3, Z_2; \mathbf{Z}\} \tag{3.1c}$$

where

$$\mathbf{Z}(z) = \begin{bmatrix} 1 & 0 \\ -z/n & 1 \end{bmatrix} \tag{3.1d}$$

and the $Z_k(p, q)$ are the Taylor expansion terms of the Hamiltonian in p^{2k}. Only the Lie–Hamilton spherical aberration coefficients Z_k^k are nonzero in free propagation (and they have a negative sign). In the paraxial regime, free propagation is approximated by the linear transformation $(p, q + zp/n + \cdots)$ that is generated by $\exp[-1/2(z/n)\{p^2, \circ\}]$. To third, fifth, and seventh aberration orders, we keep terms up to Z_2, Z_3, and Z_4, respectively. Above, the free-propagation parameter z is dimensionless; units can be made explicit in terms of a unit of length l replacing $z = z^*/l$.

A refracting line $z = \zeta(q)$ between two homogeneous media of refractive indices n_1 and n_2 that is a polynomial

$$\zeta(q) = \zeta_2 q^2 + \zeta_4 q^4 + \zeta_6 q^6 + \zeta_8 q^8 + \cdots, \tag{3.2}$$

is tangent to the $z = 0$ screen at its optical center $q = 0$, and produces the phase-space map[8]

$$\mathcal{S}(n_1, n_2; \zeta) = \mathcal{G}\{\cdots, S_4, S_3, S_2; \mathbf{S}\}, \tag{3.3a}$$

where

$$\mathbf{S} = \begin{bmatrix} 1 & g \\ 0 & 1 \end{bmatrix} \tag{3.3b}$$

characterizes the paraxial part as of Gaussian power $g = 2(n_2 - n_1)\zeta_2$. Gaussian power is the inverse of the focal length of the refracting line; when the latter is measured in units of length l, the former can be rewritten as $g = g^* l$, with g^* in units of inverse length. The dimensionless refracting surface (3.2) acquires units of the fundamental length as $\zeta^*(q^*) = \zeta_2^* q^{*2} + \zeta_4^* q^{*4} + \cdots = l\zeta(q)$, where $\zeta_2^* = \zeta_2/l$, $\zeta_4^* = \zeta_4/l^3$, etc.

The third-order aberration polynomial is

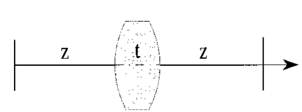

Fig. 2. Fractional Fourier transformer built as a symmetric optical arrangement with a thick lens (optical length t) between the object and screen planes (at distances z). The (circular) surfaces of the lens will be corrected to a polynomial shape $\zeta(q)$.

$$S_2(p, q) = 0p^4 + 0p^3 q + \frac{1}{2}\left(\frac{1}{n_2} - \frac{1}{n_1}\right)\zeta_2 p^2 q^2 - 2\frac{n_2 - n_1}{n_2}\zeta_2^2 p q^3 + (n_2 - n_1) \times \left(2\frac{n_2 - n_1}{n_2}\zeta_2^3 - \zeta_4\right) q^4. \tag{3.4}$$

We shall not write out the fifth- and seventh-order aberration polynomials (these can be found in Ref. 4) but note only that $S_k(p, q)$ contains the summand $(n_1 - n_2)\zeta_{2k} q^{2k}$. (The results in Refs. 4 and 8 are for three-dimensional optics; the 2-D case here applies for meridional rays, where $\mathbf{p} \cdot \mathbf{q} = pq$.)

We now concatenate the five elements of the lens arrangement: in air ($n_1 = 1$) a lens of thickness τ with refractive index $n_2 = n$ and hence optical length $t = \tau/n$, bounded by two symmetric refracting lines (3.2) of Gaussian power $g = 2(n - 1)\zeta_2 = 2(1 - n)(-\zeta_2)$, placed at distances z from the object and image lines, is

$$\mathcal{A}(z, n;\ \alpha) = \mathcal{Z}(z, 1)\mathcal{S}(1, n;\ \zeta)\mathcal{Z}(\tau, n)\mathcal{S}(n,\ 1;\ -\zeta)\mathcal{Z}(z, 1). \tag{3.5a}$$

The paraxial part

$$\mathbf{A}(z, n;\ \alpha) = \begin{bmatrix} 1 & 0 \\ -z & 1 \end{bmatrix}\begin{bmatrix} 1 & g \\ 0 & 1 \end{bmatrix}\begin{bmatrix} 1 & 0 \\ -t & 1 \end{bmatrix}\begin{bmatrix} 1 & g \\ 0 & 1 \end{bmatrix}\begin{bmatrix} 1 & 0 \\ -z & 1 \end{bmatrix} = \begin{bmatrix} 1 - gt - 2gz + g^2 zt & g(2 - gt) \\ -2z - t + 2z^2 g + 2gzt - g^2 z^2 t & 1 - gt - 2gz + g^2 zt \end{bmatrix}, \tag{3.5b}$$

is the fractional Fourier transform matrix (2.2a) provided that certain relations hold among α, g, z, and t: the (1, 1) and (2, 2) matrix elements of Eq. (3.5b) must be $\cos\alpha$, and the (1, 2) element yields the relation $g(2 - gt) = -\sin\alpha$. When we specify the desired Fourier transform angle $0 < \alpha < \pi$ and the Gaussian power g of each refracting line, the other two parameters are determined by

$$z = \frac{1}{g} + \cot\frac{\alpha}{2}, \qquad \frac{\tau}{n} = t = \frac{\sin\alpha + 2g}{g^2}. \tag{3.6}$$

For the quantities with units $z^* = lz$, $t^* = lt$, and $g^* = l^{-1}g$ marked by asterisks, the above relations will be written with the unit l in front of $\cot 1/2\alpha$ and l^{-1} in front of $\sin\alpha$. This optical arrangement provides α-fractional Fourier transforms where the points of phase space (p_α, q_α) trace out circles; it contains the limitation, however, that the free-propagation parameters (3.6) be positive and finite ($0 < z, t < \infty$). For positive powers $g > 0$, the lower limit of α is zero (the cotangent becomes infinite, and $z \to \infty$), and the upper limit is that $\alpha_{\max}$ which leads either to $z \to 0^+$ by $\alpha_{\max} = 2\pi - 2\arctan g > \pi$ or to $t \to 0^+$ by $\alpha_{\max} = \pi + \arcsin 2g > \pi$; the latter is not a limitation for $g > 1/2$.

We consider first an uncorrected transformer built with symmetric circular refracting lines $z = \pm\zeta_r(q)$ of radius r,

$$\zeta_r(q) = r - \sqrt{r^2 - q^2} \simeq \frac{q^2}{2r} + \frac{q^4}{8r^3} + \frac{q^6}{16r^5} + \frac{5q^8}{128r^7} + \cdots, \tag{3.7}$$

whose Gaussian power is $g = (n - 1)/r$, whereas the physical radius is $r^* = rl$. We now define units by choosing $r = 1$, so that $\zeta_2 = 1/2$. In the computations that follow, we also choose the value $n = 1.5$ for the refractive index of the lens, so the Gaussian power of each of its lines is fixed to $g = 1/2$.

The correction condition (2.13) to third aberration order, when written in terms of all symbolic parameters in Eqs. (3.5), is quite long [but can be handled conveniently with symbolic computation algorithms of MEXLIE (Ref. 3)]. Once numerical values are inserted, the condition (2.13) becomes a simple linear equation that determines the value of the quartic coefficient ζ_4 of the polynomial refracting line (3.2). This is inserted into Eq. (3.5a), and the process is repeated for the fifth and seventh aberration orders. To check that this program yields cogent results as we increase the aberration order, in Fig. 3 we show the $\alpha = 1/2\pi$ uncorrected Fourier transform map of phase space (produced by a lens of circular refracting lines), computed to third, fifth, and seventh aberration orders, and their corresponding corrected systems (with lenses of polynomial shape) for these orders. This shows first that the aberration expansion converges appropriately in a phase-space patch and second that the lens correction tactic indeed enlarges this patch sensibly, guaranteeing that the image grid is unslanted for $p = q$.

Figures 4 and 5 show, respectively, the phase-space transformations that are due to a family of thick-lens ar-

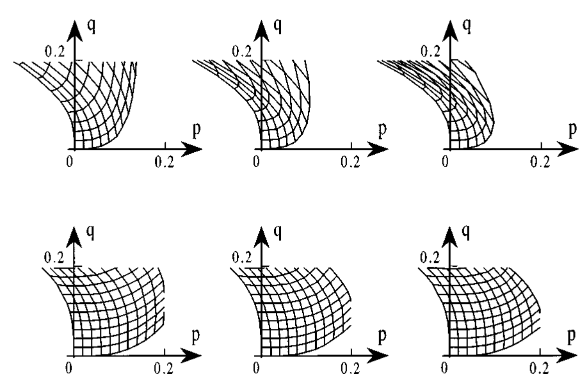

Fig. 3. Phase-space maps (in the interaction picture) of Fourier transformers ($\alpha = \frac{1}{2}\pi$) built with a symmetric lens. Top row: uncorrected system with circular refracting line ($r = 1$) computed to third, fifth, and seventh aberration orders; bottom row: corrected systems with polynomial-line lenses to the same aberration orders.

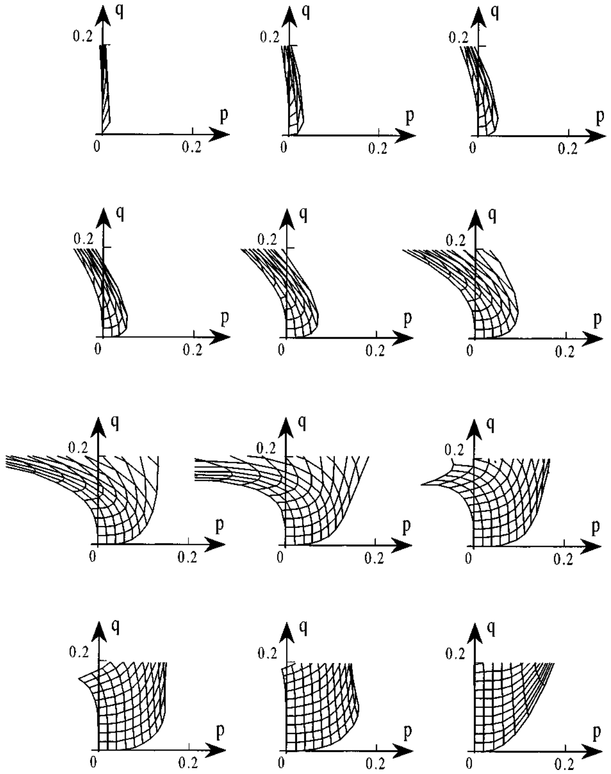

Fig. 4. Phase-space maps of an uncorrected lens fractional Fourier transformer (with circular refracting lines) for $\alpha = 15°, 30°, 45°,\ldots,180°$, computed to seventh aberration order.

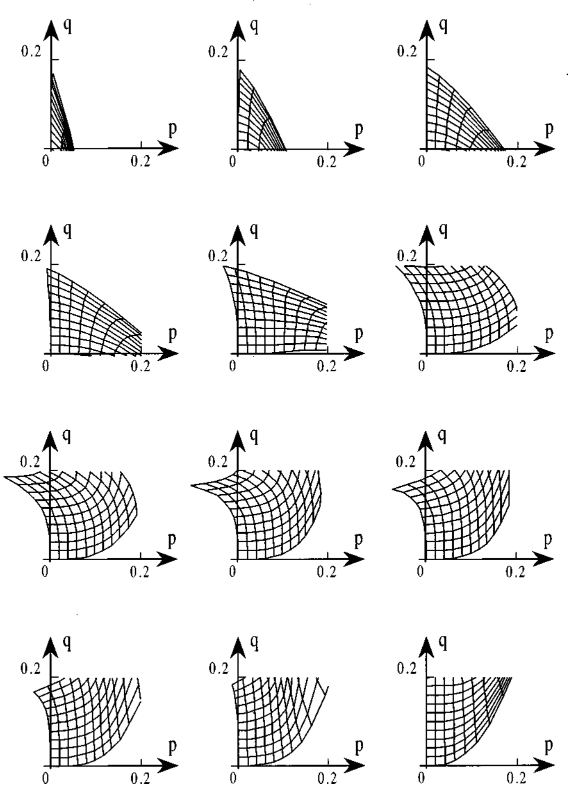

Fig. 5. Corrected fractional Fourier transform map of phase space (with the polynomial lens coefficients of Table 1) for $\alpha = 15°, 30°, 45°,\ldots, 180°$, to seventh aberration order.

rangements, uncorrected (with circular lines) and corrected (with eighth-degree polynomial lines), computed to seventh aberration order. The polynomial coefficients for circular refracting lines are $\zeta_2 = 1/2$ (paraxial standard), $\zeta_4 = 1/8 = 0.125$, $\zeta_6 = 1/16 = 0.0625$, and $\zeta_8 = 5/128 = 0.039062$. Table 1 gives the lens polynomial coefficients ζ_4, ζ_6, and ζ_8 for the corrected lens fractional Fourier transformer.

Comparing Figs. 4 and 5, the parameters z and t in Eqs. (3.6) of the physical arrangement, and the polynomial parameters in Table 1, we can conclude that lens correction is appropriate for angles α equal to or greater than 60°, including the Fourier transform ($\alpha = 90°$), the inverted imager ($\alpha = 180°$), and beyond, to the inverse Fourier transformer ($\alpha = 270°$) (not shown here) in a sensibly larger patch of phase space. For smaller transform angles α, the free flight distance z becomes very large [cf. Eqs. (3.6)], and the aberration expansion itself appears to be unreliable. From Table 1 we note that the polynomial coefficients vary smoothly with α and peak at $\alpha = 165°$. Note that for the Fourier transformer ($\alpha = 90°$), the corrected refracting lines are very close to the parabolas $\zeta_2 q^2$.

4. WAVEGUIDE ARRANGEMENT

A 2-D inhomogeneous optical medium characterized by the z-independent refractive index

$$\begin{aligned} n_e(q) &= (\nu^2 - \mu^2 q^2)^{1/2} \\ &= \nu - \frac{\mu^2}{2\nu} q^2 - \frac{\mu^4}{8\nu^3} q^4 - \frac{\mu^6}{16\nu^5} q^6 - \cdots \quad (4.1) \end{aligned}$$

is what we call an elliptic-index-profile waveguide. In the paraxial regime, the index profile is approximated by the quadratic term and is commonly known as parabolic. A length of such a medium, as shown in Fig. 6, performs

Table 1. Coefficients of the Polynomial Refracting Line That Correct the Lens Arrangement for Fractional Fourier Transformation of Angle α in Steps of 15° to Third, Fifth, and Seventh Aberration Orders

Fourier Angle α (deg)	Polynomial Line Parameters		
	ζ_4	ζ_6	ζ_8
15	−0.0159	0.0213	−0.0211
30	−0.0303	0.0179	−0.0152
45	−0.0350	0.0087	−0.0022
60	−0.0310	−0.0010	−0.0025
75	−0.0183	−0.0044	−0.0070
90	0.0000	0.0000	−0.0062
105	0.0194	0.0115	0.0063
120	0.0428	0.0153	0.0701
135	0.0782	0.0515	0.2703
150	0.1264	−0.3021	1.3753
165	0.1786	−0.6600	5.3782
180	0.0816	0.0250	0.0098

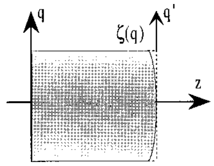

Fig. 6. A length of a graded-index medium (a waveguide) acts as an (aberrating) fractional Fourier transformer. The correction tactic is applied to warp the output screen to a polynomial shape $\zeta(q)$.

an (aberrated) fractional Fourier transform; below we will correct this arrangement, as much as possible, by warping the screen.

Propagation along the optical z axis is generated as in Eq. (3.1b) but by the q-dependent Hamiltonian of the profile (4.1). The evolution of phase space along this axis through a distance z is given by the exponentiated Lie–Poisson operator

$$\begin{aligned}\mathcal{E}(\nu, \mu; z) &= \exp[z\{(\nu^2 - p^2 - \mu^2 q^2)^{1/2}, \circ\}] \\ &= \cdots \times \exp\left[\frac{-z}{8\nu^3}\{(p^2 + \mu^2 q^2)^2, \circ\}\right] \\ &\quad \times \exp\left(\frac{-z}{2\nu}\{p^2 + \mu^2 q^2, \circ\}\right) \qquad (4.2a) \\ &= \mathcal{G}\{\cdots, E_2; \mathbf{E}(z)\}, \qquad (4.2b)\end{aligned}$$

where

$$\mathbf{E}(z) = \begin{bmatrix} \cos\dfrac{\mu z}{\nu} & \mu \sin\dfrac{\mu z}{\nu} \\ -\dfrac{1}{\mu}\sin\dfrac{\mu z}{\nu} & \cos\dfrac{\mu z}{\nu} \end{bmatrix} \qquad (4.2c)$$

is the paraxial part. The third-order aberration polynomial is

$$\begin{aligned}E_2(p, q; z) &= -(z/8\nu^3)p^4 - (z\mu^2/4\nu^3)p^2q^2 \\ &\quad - (z\mu^4/8\nu^3)q^4, \qquad (4.2d)\end{aligned}$$

and generally $E_k(p, q; z) \sim -z\nu^{-k-1}(p^2 + \mu^2 q^2)^k$. We define units of length so that $\mu = 1$, to have the circular motion of phase space shown in the figures.

The action of Eqs. (4.2) on phase space can be expressed in closed form, moreover, by noting that the Hamiltonian flow lines are the nested ellipses $p^2 + \mu^2 q^2 =$ constant. For $\mu = 1$ they are the circles

$$\mathcal{E}(\nu; z)\begin{pmatrix} p \\ q \end{pmatrix} = \begin{bmatrix} \cos\kappa z & -\sin\kappa z \\ \sin\kappa z & \cos\kappa z \end{bmatrix}\begin{pmatrix} p \\ q \end{pmatrix} = \begin{pmatrix} P(p, q; z) \\ Q(p, q; z) \end{pmatrix}, \qquad (4.3a)$$

where the oscillation frequency $\kappa = \kappa(p, q)$ depends on their radius:

$$\begin{aligned}\kappa(p, q) &= \frac{1}{[\nu^2 - (p^2 + q^2)]^{1/2}} = \frac{1}{\nu} + \frac{1}{2\nu^3}(p^2 + q^2) \\ &\quad + \frac{3}{8\nu^5}(p^2 + q^2)^2 + \cdots. \qquad (4.3b)\end{aligned}$$

The paraxial oscillation frequency is $\kappa_0 = \kappa(0, 0) = \mu/\nu$ at the center of phase space [cf. Eqs. (4.2b), (4.2c), and (4.3b)]. In the metaxial regime, this system becomes dispersive, since phase space rotates differentially, with larger circles moving faster; the represented rays in the waveguide go through larger angles and elongations, up to where the refractive index $n_e(q_{\max})$ drops to zero. The oscillation frequency (4.3b) is real inside the boundary circle $p^2 + q^2 = \nu^2$, but physically realizable rays must lie inside the smaller circle $p^2 + q^2 = \nu^2 - 1$ because $n = 1$ corresponds to vacuum.

Paraxially, a length z of the waveguide is a fractional Fourier transformer by the negative angle $\alpha = -z/\nu$, as can be seen by comparing the matrix elements of Eqs. (2.2) and (4.2). Graded-index elements are therefore inverse Fourier transformers. Figure 7 is the waveguide analog of Fig. 3; it shows the maps of phase space produced by an uncorrected $\alpha = -\frac{1}{2}\pi$ (inverse) Fourier transformer, computed to third, fifth, and seventh aberration orders,[3] and the maps produced with the corrected optical arrangement proposed below. Note that the phase-space patch shown is much larger than that in the lens arrangement. As in the previous figures, the rigid paraxial rotation has been factored out from expression (4.2b). Figure 8 shows the fractional Fourier transform maps obtained from the simple (uncorrected) elliptic-index-profile waveguide, computed with MEXLIE to seventh aberration order. This phase-space map is unsatisfactory principally because of the inclination of the mapped grid at the q axis, which indicates that there will be strong unfocusing of the images away from the optical center.

To correct the waveguide arrangement, we propose to warp the output face of the waveguide, so that the photographic paper or the line of sensors that define the image screen is no longer straight but a polynomial line (3.2), where we can adjust the polynomial coefficients $\zeta_2, \zeta_4, \ldots$. To formulate and compute this correction, we use the canonical phase-space transformation from a flat to a warped reference screen, called the root map, as studied in Ref. 9. (This was introduced earlier for waveguides in Ref. 10 and is implemented in MEXLIE). Under the root map $\mathcal{R}(n_e; \zeta)$, the position coordinate q is mapped to the impact point $\bar{q}$ of the ray (p, q) on the line $z = \zeta(\bar{q})$ in the inhomogeneous optical medium (4.1). This is

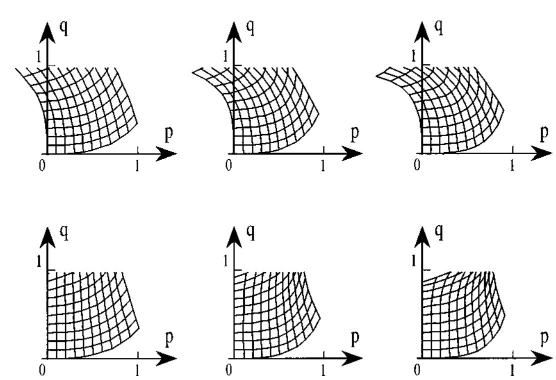

Fig. 7. Phase-space maps (in the interaction picture) of a (an inverse) Fourier transformer ($\alpha = -\frac{1}{2}\pi$) built with an elliptic-index-profile waveguide. Top row: computation to third, fifth, and seventh aberration orders; Bottom row: corrected map to the same aberration orders.

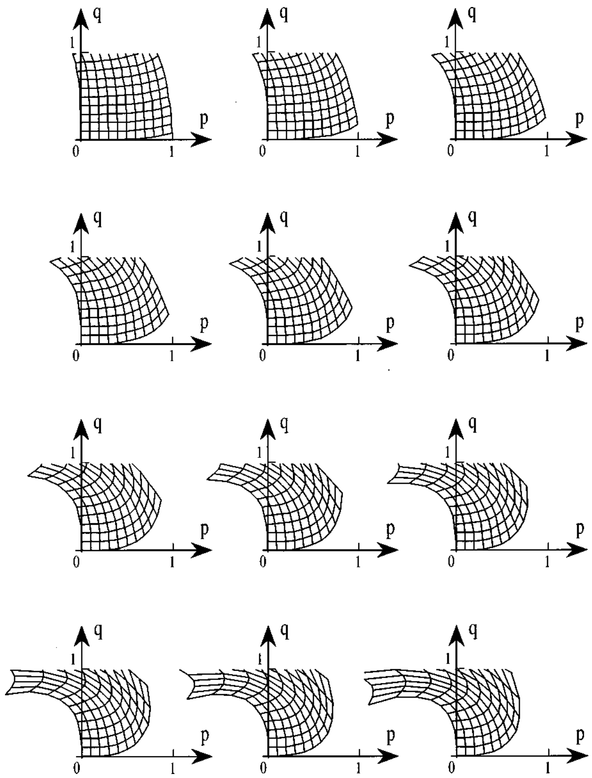

Fig. 8. Uncorrected waveguide arrangement for fractional Fourier transformation (in the interaction picture) for $\alpha = 15°, 30°, 45°, \ldots, 180°$, to seventh aberration order.

$$\bar{q} = \mathcal{R}(n_e;\,\zeta), \quad q = Q(p, q;\, \zeta(\bar{q})), \tag{4.4a}$$

and the canonically conjugate momentum is of the form[10]

$$\bar{p} = \mathcal{R}(n_e;\,\zeta), \quad p = P(p, q;\, \zeta(\bar{q})) + [\nu^2 - (p^2 + q^2)]^{1/2} \frac{d\zeta(\bar{q})}{d\bar{q}}. \tag{4.4b}$$

Note that Eq. (4.4a) is an implicit equation that yields $\bar{q}$ by polynomial expansion in a Taylor series; once $\bar{q}(p, q)$ has been found, its replacement in Eq. (4.4b) yields $\bar{p}(p, q)$ explicitly. The root transformation can be written as

$$\mathcal{R}(n_e;\,\zeta) = \mathcal{G}\{\cdots, R_3, R_2;\, \mathbf{R}\}, \tag{4.5a}$$

where

$$\mathbf{R} = \begin{bmatrix} 1 & -2\nu\zeta_2 \\ 0 & 1 \end{bmatrix} \tag{4.5b}$$

is the paraxial part, the third-order aberration polynomial is

$$R_2(p, q) = -(\zeta_2/2\nu)p^2q^2 + (\nu\zeta_4 - \zeta_2/2\nu)q^4, \tag{4.5c}$$

and the fifth- and seventh-order polynomials can be found in Ref. 10. It is called the root map because it factors the transformation that is due to a refracting line between two media n_1 and n_2 into $\mathcal{S}(n_1, n_2;\,\zeta) = \mathcal{R}(n_1;\,\zeta) \times [\mathcal{R}(n_2;\,\zeta)]^{-1}$.

Now we can compute the corrected fractional Fourier transformer built out of a waveguide that is capped on the output side with a warped face:

$$\mathcal{A}(z, n_e;\,\alpha) = \mathcal{E}(n_e;\,z)\mathcal{R}(n_e;\,\zeta). \tag{4.6}$$

Multiplying the paraxial parts, we see that $\mathcal{A}(z, n_e;\,\alpha)$ maintains its paraxial rotation form (2.2) only when $\zeta_2 = 0$ in Eq. (3.2), i.e., when the exit surface (line) is

Table 2. Coefficients of the Polynomial Exit Sensor Line That Correct the Waveguide Arrangements for Fractional Fourier Transformation of Angle α in Steps of 15° to Third, Fifth, and Seventh Aberration Orders[a]

Fourier Angle $-\alpha$ (deg)	Polynomial Line Parameters		
	$-\zeta_4$	$-\zeta_6$	$-\zeta_8$
15	0.0097	0.0043	0.0018
30	0.0194	0.0086	0.0038
45	0.0291	0.0129	0.0060
60	0.0388	0.0172	0.0086
75	0.0485	0.0215	0.0117
90	0.0582	0.0259	0.0155
105	0.0679	0.0302	0.0201
120	0.0776	0.0345	0.0256
135	0.0873	0.0388	0.0321
150	0.0970	0.0431	0.0398
165	0.1067	0.0474	0.0489
180	0.1164	0.0517	0.0594

[a] The values of α and ζ_{2k} are negative: the transforms are *inverse*, and the exit face of the waveguide is convex.

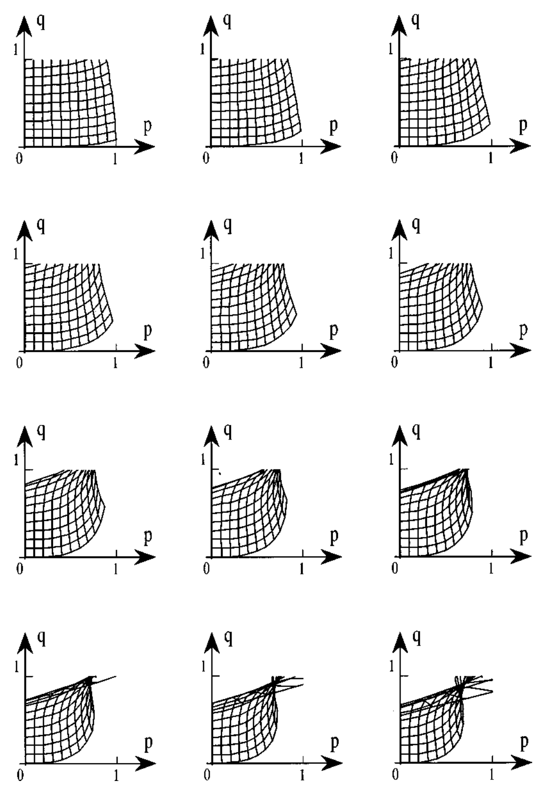

Fig. 9. Waveguide arrangement for fractional Fourier transformation corrected by warping the exit sensor line so that there is spherical aberration (in the interaction picture) to seventh aberration order for transform angles of $\alpha = 15°, 30°, 45°, \ldots, 180°$.

paraxially straight. We can therefore use only quartic- and higher-degree polynomial lines to correct the waveguide fractional Fourier transformer. When $\zeta_2 = 0$, the third-order aberration polynomial (4.5c) reduces to $R_2(p, q) = \nu\zeta_4 q^4$, and the 5-vector of third-order aberration coefficients of the waveguide to be corrected is

$$A_2 = E_2 + \mathbf{D}^{(2)}(\mathbf{\Phi}(\alpha))R_2, \tag{4.7}$$

where E_2 is the vector of uncorrected third-order aberration coefficients of the waveguide [Eq. (4.2d)], $\mathbf{D}^{(2)}(\mathbf{\Phi}(\alpha))$ is the 5×5 matrix representation of the rotation [Eq. (2.2)], and the column vector R_2 contains the aberration coefficients in the polynomial (4.5c) that is due to the warped screen line with $\zeta_2 = 0$, namely, $(0, 0, 0, 0, \nu\zeta_4)$. We recall that $z = -\nu\alpha \geqslant 0$ and note the D-matrix elements $D^{(2)}_{2,2}(\alpha) = \cos^4\alpha = D^{(2)}_{-2,-2}(\alpha)$ and $D^{(2)}_{2,-2}(\alpha) = \sin^4\alpha = D^{(2)}_{-2,2}(\alpha)$. From Eq. (4.7) we thus find the third-order aberration coefficients of $\mathcal{A}(z, n_e;\, \alpha)$ in the interaction frame:

$$A^2_2 = -(\alpha/8\nu^2) + \nu\zeta_4 \sin^4\alpha, \tag{4.8a}$$

$$A^2_0 = -(\alpha/4\nu^2) + 6\nu\zeta_4 \sin^2\alpha\cos^2\alpha, \tag{4.8b}$$

$$A^2_{-2} = -(\alpha/8\nu^2) + \nu\zeta_4 \cos^4\alpha, \tag{4.8c}$$

and $A^2_1 = 0 = A^2_{-1}$.

To correct the waveguide arrangement for fractional Fourier transformation, we now enter the coefficients (4.8) into Eqs. (2.10). If we were to demand orthogonality on a line of the map through Eq. (2.13) as in Section 3, we would obtain $\zeta_4 = 0$, etc., and no correction. Our tactic instead will be to set spherical aberration to zero [$A^2_2 = 0$ (in the interaction frame)], because then the image of the q axis will be *on* the q axis to third aberration order by Eqs. (2.10). Thus, for fixed transform angle $\alpha < 0$ and refractive index ν at the center of the waveguide, Eq. (4.8a) determines the quartic warp coefficient $\zeta_4 < 0$ by a linear equation. Once ζ_4 is found, the computation is performed to fifth aberration order with the sextic warp coefficient ζ_6, which appears only in the R^3_{-3} coefficient of the root transformation (4.4) and does so linearly; ζ_6 is thus determined by $A^3_3 = 0$, a linear equation. Similarly, seventh-order spherical aberration is eliminated, and this determines ζ_8. These coefficients are given in Table 2; they are negative, so the exit face of the corrected waveguide is convex. Both ζ_4 and ζ_6 grow linearly with α. In Fig. 9 we show the phase-space map of the waveguide corrected to have no spherical aberration, to seventh aberration order.

On the basis of Figs. 8 and 9, we conclude that waveguide arrangements to produce (inverse) fractional Fourier transforms are adequate in a much larger coordinate patch and while the waveguide is short, i.e., for values of $|\alpha|$ up to 60°. Correction by a warped exit face extends this range well beyond 90°.

5. FRACTIONAL TRANSFORMS IN WAVE OPTICS; CONCLUSIONS

The embedding of the Fourier transform into a continuous group of integral transforms has been of wide interest in mechanics and in optics. The first explicit and rather complete treatment of this group of transformations appears to have been written by Condon in Ref. 11 (in 1937) and thereafter apparently forgotten by most researchers. As a problem in quantum mechanics, the phase-space evolution of systems with quadratic Hamiltonians is linear and was determined by Moshinsky and Quesne in 1970.[12] These canonical transforms form the group $\mathrm{SL}(2, \mathbb{R}) = \mathrm{Sp}(2, \mathbb{R})$ and can be extended to a subsemigroup of 2×2 matrices that include the Bargmann transform to creation and annihilation operators.[13] In 1980 Namias[14] found the same integral kernel as a generating function of Hermite polynomials. The relevance of this group for first-order optics was realized in 1980 by Nazarathy and Shamir.[15] For nonaxisymmetric linear systems in N dimensions, the relevant group is the symplectic $\mathrm{Sp}(2N, \mathbb{R})$.[16]

Fractional Fourier transformation was specifically addressed and used for information processing by Mendlovic, Ozaktas, and many of their collaborators from 1993.[17] It is currently used in various contexts for asymptotic expansion of wave propagators[18] and the problem of phase retrieval of the signal and diffractive phase elements.[19]

Geometric wave optics and scalar wave optics are homomorphic theories in the paraxial regime; N-dimensional axisymmetric optical systems are represented by 2×2 matrices of unit determinant. In wave optics these systems act through unitary integral kernels on the Hilbert space $\mathcal{L}^2(\mathbb{R})$ of input wave functions of position q. The kernels represent the exponentials of self-adjoint operators of the form $a\hat{p}^2 + b\{\hat{p}\hat{q}\}_+ + c\hat{q}^2$, where $\hat{p} = -i(\lambda/2\pi)\partial/\partial q$ and $\hat{q} = q\,\cdot$ are the usual wave-optical operators of momentum and position for wavelength λ and $\{\circ\}_+$ is the anticommutator. Geometric and wave theories also maintain their correspondence under the nonlinear Lie–Hamilton transformations (2.5) generated exclusively by the functions $f(p)$ and $qg(p)$ (generic spherical aberration and coma) or by the functions $f(q)$ and $pg(q)$ (pocus and distortion)—but not under the composition of these two algebras.[20] When generic aberrations occur, the correspondence between geometric and wave theories becomes complicated. One result that brings some order into the problem is that the correspondence is maintained, under linear transformations, between $A_k(p, q)$ [the aberration polynomial (2.6) of rank $k > 1$] and the Weyl-ordered operator $\{A_k(\hat{p}, \hat{q})\}_W$ *only*.[21] (The Weyl order of the operator factors of a monomial is the sum of all their possible permutations as individual objects divided by the factorial of their number.)

The strategy in this paper has been to separate the linear and aberration (interaction) parts in Eq. (2.4) and propose two tactics to minimize the latter for lens and waveguide fractional Fourier transformers. Through enlarging the region of phase space where the geometric map is close to linearity, we may expect that the corresponding wave-optical systems will follow relation (2.9) and Eqs. (2.14) and (2.15) to third, fifth, and seventh orders when the same geometric aberration polynomials are replaced by their corresponding Weyl-ordered operators. In a future paper, we hope to show that this is indeed the case by means of the Wigner distributions of the input and output waveforms.[22]

ACKNOWLEDGMENTS

We acknowledge support from project DGAPA–UNAM IN-106595 (Optica Matemática) and collaboration from Ana Leonor Rivera.

Address correspondence to Kurt Bernardo Wolf at the location on the title page; by phone, 52-73-17-3388; or by e-mail, bwolf@ce.ifisicam.unam.mx.

REFERENCES

1. K. B. Wolf, "The Fourier transform in metaxial geometric optics," J. Opt. Soc. Am. A **8**, 1399–1403 (1991).
2. V. I. Man'ko and K. B. Wolf, "The map between Heisenberg–Weyl and Euclidean optics is comatic," in *Lie Methods in Optics*, Vol. 352 of Lecture Notes in Physics, J. Sánchez-Mondragón and K. B. Wolf, eds. (Springer-Verlag, Heidelberg, 1989), Chap. 7, pp. 163–197.
3. K. B. Wolf and G. Krötzsch, "MEXLIE 2, a set of symbolic computation functions for geometric aberration optics," Manuales IIMAS–UNAM (Instituto de Investigaciones en Matemáticas Aplicadas y en Sistemas, Universidad Nacional Autónoma de México) No. 10 (June, 1995).
4. A. J. Dragt, E. Forest, and K. B. Wolf, "Foundations of a Lie algebraic theory of geometrical optics," in *Lie Methods in Optics*, Vol. 250 of Lecture Notes in Physics (Springer-Verlag, Heidelberg, 1986), Chap. 4, pp. 105–158.
5. A. J. Dragt and J. Finn, "Lie series and invariant functions for analytic symplectic maps," J. Math. Phys. (N.Y.) **17**, 2215–2227 (1976); A. J. Dragt, "Lie algebraic theory of geometric optics and optical aberrations," J. Opt. Soc. Am. **72**, 372–379 (1982); S. Steinberg, "Factored product expansions of nonlinear differential equations," SIAM (Soc. Ind. Appl. Math.) J. Math. Anal. **15**, 108–115 (1984); S. Steinberg, "Lie series, Lie transformations, and their applications," in *Lie Methods in Optics*, Vol. 250 of Lecture Notes in Physics (Springer-Verlag, Heidelberg, 1986), Chap. 3, pp. 45–102.
6. K. B. Wolf, "Symmetry-adapted classification of aberrations," J. Opt. Soc. Am. A **5**, 1226–1232 (1988).
7. H. Buchdahl, *Optical Aberration Coefficients* (Dover, New York, 1968).
8. M. Navarro-Saad and K. B. Wolf, "Factorization of the phase-space transformation produced by an arbitrary refracting surface," J. Opt. Soc. Am. A **3**, 340–346 (1986).
9. E. J. Atzema, G. Krötzsch, and K. B. Wolf, "Canonical transformations to warped surfaces: correction of aberrated optical images," J. Phys. A **30**, 5793–5803 (1997).
10. K. B. Wolf, "Refracting surfaces between fibers," J. Opt. Soc. Am. A **8**, 1389–1398 (1991).
11. E. U. Condon, "Immersion of the Fourier transform in a continuous group of functional transforms," Proc. Natl. Acad. Sci. USA **23**, 158–164 (1937).
12. M. Moshinsky and C. Quesne, "Oscillator systems," in *Proceedings of the XVth Solvay Conference in Physics*, E. Progogine, ed. (Gordon & Breach, New York, 1974); C. Quesne and M. Moshinsky, "Linear canonical transformations and their unitary representations," J. Math. Phys. (N.Y.) **12**, 1772–1780 (1971); M. Moshinsky and C. Quesne, "Canonical transformations and matrix elements," J. Math. Phys. (N.Y.) **12**, 1780–1783 (1971).
13. K. B. Wolf, "Canonical transforms. I. Complex linear transforms," J. Math. Phys. (N.Y.) **15**, 1295–1301 (1974); K. B. Wolf, *Integral Transforms in Science and Engineering* (Plenum, New York, 1979), Chap. 9.
14. V. Namias, "The fractional Fourier transform and its application in quantum mechanics," J. Inst. Math. Appl. **25**, 241–265 (1980).
15. M. Nazarathy and J. Shamir, "Fourier optics described by operator algebra," J. Opt. Soc. Am. **70**, 150–158 (1980).
16. O. Castaños, E. López Moreno, and K. B. Wolf, "Canonical transforms for paraxial wave optics," in *Lie Methods in Optics*, Vol. 250 of Lecture Notes in Physics (Springer-Verlag, Heidelberg, 1986), Chap. 5, pp. 159–182.
17. D. Mendlovic and H. M. Ozaktas, "Fractional Fourier transforms and their implementations. I," J. Opt. Soc. Am. A **10**, 1875–1881 (1993); H. M. Ozaktas and D. Mendlovic, "Fractional Fourier transforms and their implementations. II," J. Opt. Soc. Am. A **10**, 2522–2531 (1993); H. M. Ozaktas and D. Mendlovic, "Fractional Fourier transform of fractional order and their optical interpretation," Opt. Commun. **101**, 163–169 (1993); H. M. Ozaktas and D. Mendlovic, "Fractional Fourier optics," J. Opt. Soc. Am. A **12**, 743–750 (1995); D. Mendlovic, Y. Bitran, R. G. Dorsch, and A. W. Lohmann, "Optical fractional correlation: experimental results," J. Opt. Soc. Am. A **12**, 1665–1670 (1995).
18. M. A. Alonso and G. W. Forbes, "Uniform asymptotic expansion for wave propagators via fractional transformations," J. Opt. Soc. Am. A **14**, 1279–1292 (1997).
19. B.-Zh. Dong, Y. Zhang, B.-Y. Gu, and G.-Zh. Yang, "Numerical investigation of phase retrieval of a fractional Fourier transform," J. Opt. Soc. Am. A **14**, 2709–2714 (1997); Y. Zhang, B.-Zh. Dong, B.-Y. Gu, and G.-Zh. Yang, "Beam shaping in the fractional Fourier transform domain," J. Opt. Soc. Am. A **15**, 1114–1120 (1998).
20. K. B. Wolf, "The Heisenberg–Weyl ring in quantum mechanics," in *Group Theory and Its Applications, III*, E. M. Loebl, ed. (Academic, New York, 1975), pp. 189–247.
21. M. García-Bullé, W. Lassner, and K. B. Wolf, "The metaplectic group within the Heisenberg–Weyl ring," J. Math. Phys. (N.Y.) **27**, 29–36 (1986).
22. A. L. Rivera, N. M. Atakishiyev, S. M. Chumakov, and K. B. Wolf, "Evolution under polynomial Hamiltonians in quantum and optical phase spaces," Phys. Rev. A **55**, 876–889 (1997).